Deprotonation Dynamics and Stokes Shift of Pyranine (HPTS)

D. B. Spry, A. Goun, and M. D. Fayer*

Department of Chemistry, Stanford University, Stanford, California 94305

Received: September 15, 2006; In Final Form: November 14, 2006

The short and intermediate time scale dynamics of the photoacid pyranine (1-hydroxy-3,6,8-pyrenetrisulfonic acid, commonly referred to as HPTS) are studied with visible pump−probe spectroscopy in various solvents to elucidate the nature of its proton-transfer kinetics in water. The observed time dependences of HPTS are compared with those of the methoxy derivative, MPTS. A global fitting procedure is employed to model both the spectral shift (Stokes shift) caused by solvent reorganization and deprotonation of pyranine in water. Three distinct time-dependent features can be clearly identified. They are the Stokes shift (1 ps in H_2O and 1.5 ps in D_2O), followed by the deprotonation processes, which gives rise to a biexponential decay of the protonated species with time constants (in H_2O) of 3 and 88 ps. By the use of a model previously discussed in the literature, the biexponential process can be interpreted as an initial deprotonation step followed by the longer time scale process which separates the resulting ion pair. The results presented here are consistent with some of the previous reports but unambiguously identify and quantitatively measure the Stokes shift as a separate and distinct phenomenon from the deprotonation process, in contrast to other reports that have suggested that all short time (a few picoseconds) dynamics are merely a Stokes shift.

I. Introduction

Photoacids, or molecules with an electronically excited-state pK_a much lower than that of the ground state, have proven to be immensely valuable for studying both proton-transfer and hydrogen-bonding dynamics in water.[1,2] Because the time scale for a typical proton-transfer reaction is often on the order of picoseconds or femtoseconds, they are difficult to follow under equilibrium conditions. However, because both the electronic absorption and emission spectra of photoacids change dramatically upon deprotonation the time-dependent spectra of photoacids can be used in conjunction with an ultrafast excitation source to monitor the course of a proton-transfer reaction in real time.

One of the most widely used photoacids for the study of diffusion-controlled proton-transfer dynamics in an aqueous environment is 8-hydroxypyrene-1,3,6-trisulfonate (pyranine or HPTS), which is shown in Figure 1. It is one of the earliest recognized photoacids, initially studied in the 1950s by Förster[3] and Weller.[4] However, it was not until the mid-1970s that HPTS became prominent in the study of proton-transfer dynamics. Völker and Förster[5] found the ground-state recombination kinetics with the dissociated proton to be the fastest bimolecular reaction known at the time. Because of enhanced Columbic attraction of the HPTS anion's fourfold negative charge, the reaction is nearly twice as fast as the self-neutralization of water. Approximately a decade later, Huppert[6,7] was the first to observe excited-state geminate recombination in HPTS using time-correlated single photon counting (TCSPC).

Yet another decade later, Prayer et al. used fluorescence upconversion to study previously unobserved fast time dynamics of HPTS.[8] They reported a 300 fs and 2.5 ps decay of protonated state fluorescence. The 300 fs component was attributed to a general solvation process. However, since the discovery of the intermediate dynamics (∼2.5 ps), the identity of the process that gives rise to spectral changes on the shortest time scale has had several interpretations.[8−11] Because of its potential relationship to the mechanism of proton transfer in water, substantial attention has been given to the nature of the intermediate time scale process.

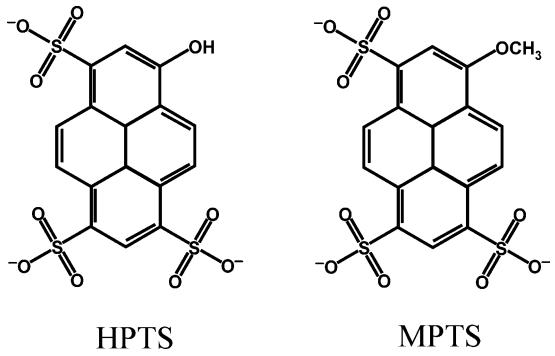

Figure 1. Structures of pyranine (1-hydroxy-3,6,8-pyrenetrisulfonic acid, commonly referred to as HPTS) and MPTS, the methoxy derivative of HPTS.

The first suggested explanation of the intermediate component[8] follows from the Eigen−Weller model for proton transfer.[12,13] Here, the intermediate time component is produced by the initial deprotonation process that forms a contact ion pair. The second step breaks contact between the two ions and is followed by diffusion.

$$\mathrm{AH\cdots B} \underset{k_{-1}}{\overset{k_1}{\rightleftharpoons}} [\mathrm{A^-\cdots HB^+}] \underset{k_{-2}}{\overset{k_2}{\rightleftharpoons}} \mathrm{A^- + HB^+} \qquad (1)$$

This mechanism was recently employed by Huppert and coworkers in a series of visible pump−probe and TCSPC studies.[11,14] They correlated the fast decay seen in the pump−probe signal to an initial offset in the TCSPC signal of the deprotonated state.[11] They further suggested that the amplitude

* To whom correspondence should be addressed. E-mail: fayer@stanford.edu.

10.1021/jp066041k CCC: $37.00
Published on Web 12/22/2006

of the intermediate time scale component is pH dependent. Both of these observations support a deprotonation mechanism to account for the ~3 ps component.[14]

There also have been suggestions of the formation of an internal charge-transfer (ICT) state instead of complete proton transfer to account for the 3 ps response. Tran-Thi was the first to give such an explanation, which was inspired by the proposed mechanism for photodissociation for a well-studied family of naphthols.[2,15−18] It was suggested that the photoacid is initially excited into a ^1L_b electronic state, which was taken to be the lowest energy excited state. Before deprotonation can occur, the excited molecule must first undergo a potential curve crossing to a nearby ^1L_a state. The crossing was thought to be controlled by the solvent reorganization time. The ^1L_a state was suspected to have the appropriate CT characteristics to enable proton transfer. The proton transfer was responsible for the 90 ps component of the optical experiments. However, recent detailed studies of the ordering of the electronic excited states of HTPS show that, in both the protonated and deprotonated forms, the ^1L_a state is the lowest energy state,[19] which rules out the curve crossing mechanism.

Recently, HPTS has been studied using visible-pump IR-probe spectroscopy.[9,20−22] Proton-transfer dynamics were monitored in H_2O and D_2O by probing the fingerprint region of the IR spectrum, which appear to change vibrational frequency upon HPTS deprotonation. In such experiments, it is likely that an electronic Stokes shift would not be evident. The longer time scale ~90 ps component observed in previous experiments is present. However, the ~3 ps component seen by visible measurements was not observed in the visible-pump IR-probe experiments. From the vis/IR experiments, the authors concluded that the intermediate component was most likely not due to proton transfer but might instead be associated with hydrogen-bonding rearrangements of the solvent or some other solvation process. However, it is not clear if the vibrational modes probed are sensitive to all steps in the deprotonation process. The strictly visible spectroscopy also has several complicating features. Nibbering and co-workers have pointed out that visible pump−probe spectra can be difficult to interpret because of overlapping transitions and the electronic states that are observed can be highly sensitive to solvent reorganization, which may interfere with observation of the proton-transfer process.[9,22]

The goal of this paper is to analyze the visible pump−probe spectra of HPTS in a global manner and definitely decouple the solvation (Stokes shift) and proton-transfer dynamics. The important question is whether the ~3 ps dynamics observed in the strictly electronic spectroscopy is just part of the Stokes shift or is it in fact the initial deprotonation step. In order to extract information regarding a Stokes shift and a possible initial deprotonation process, it is necessary to analyze more than a single frequency point. Because a Stokes shift and deprotonation produce fundamentally different time-dependent spectral responses, examining the entire spectrum as a function of time has the potential to answer the question posed above. The data and analysis presented below decomposes the time-dependent data into distinct spectral components. By testing the method on MPTS, which has a Stokes shift but does not undergo deprotonation, and HPTS in solvents that prevent deprotonation, the Stokes shift and proton-transfer components of the HPTS time dependence can be unambiguously assigned. The experiments provide accurate quantitative results that demonstrate that there is a Stokes shift with time scale of 1 ps, an initial proton-transfer step with a 3 ps time scale, and a long time scale component of the proton transfer of 90 ps. These data support previous studies[11,14] but indicate that some visible-pump IR-probe experiments[9] may not be sensitive to the initial step in the photoacid deprotonation.

II. Experimental Procedures

Pyranine (>98%) and MPTS (>98%) were purchased from Fluka. Spectroscopic grade methanol, formamide, and D_2O were purchased from Acros Inc. The water used was deionized.

UV−vis absorption spectra were measured on a Cary-6000i spectrophotometer. Fluorescence and anisotropy spectra were taken on a Fluorolog-3 fluorescence spectrometer. The fluorescence measurements were made at low concentration (below 10^{-4} M) to avoid spectral distortion from emission reabsorption. The spectra were corrected for the Xe lamp intensity profile, monochromator, and photomultiplier response.

Pump−probe experiments in which a particular wavelength is used for the pump and a continuum is used as the probe were performed using a Ti:Sapphire regenerative amplified source and a CCD detection system. The pump beam was centered at 400 nm at 7 μJ per pulse and 65 fs duration with a spot size diameter of 200 μm. A "white light" continuum, used for the probe, was generated by focusing 1−2 μJ of 800 nm light in a 1 mm cuvette of water. A half-wave plate/polarizer combination was used to attenuate the 800 nm light to give the most stable white light. The continuum generated ranged from the near-IR to somewhat beyond 390 nm and was at most 100 nJ integrated over the entire wavelength range. The white light was separated into two beams with a beam splitter. One beam was used as the probe and crossed with the pump in the sample, and the other one was used as a reference to monitor the intensity and spectral characteristics of the white light. The timing between the pump and probe was achieved by passing the pump beam down a high-resolution delay line with a ~1 fs resolution. However, because the time scales of interest ranged from picoseconds to hundreds of picoseconds, 100 fs steps were used.

The probe and reference beams were focused into two optical fibers. The outputs of the fibers are at the entrance slit of a 0.3 m monochromator. The dispersed outputs of the two input beams are detected by a 1340 × 100 pixel CCD detector. The probe and reference produce separate readout stripes on the CCD, which are used to obtain the difference absorption spectrum between pump on and pump off. The reference spectrum permits correction for variation over time of the white light characteristics.

III. Results and Discussion

A. Analysis of Stokes Shifts. Figures 2A and 3A show the experimental time-dependent pump−probe spectra of HPTS in formamide and methanol, respectively. The spectra shown in Figure 2A were taken at 100 and 600 fs and 2, 4, and 300 ps, and those shown in Figure 3A were taken at 1, 4, 9, 20, and 180 ps. In these solvents, excited-state proton transfer (ESPT) does not occur. Similar results have been observed in previous studies[11] of HPTS and by Pines and co-workers for the closely related molecule HPTA in dimethyl sulfoxide (DMSO) mixtures.[23] The trends seen in these spectra are representative of all solvents that can hydrogen bond strongly with HPTS but do not permit ESPT. Excited-state absorption, which gives a positive signal and appears around 550 nm, has a time-dependent blue shift. Stimulated emission has the opposite sign with a maximum at 440 nm and red shifts with time. This is consistent with the solvent stabilizing the first excited state over the ground or second excited state, which is to be expected because the solvent is responding to the generation of the first excited state.

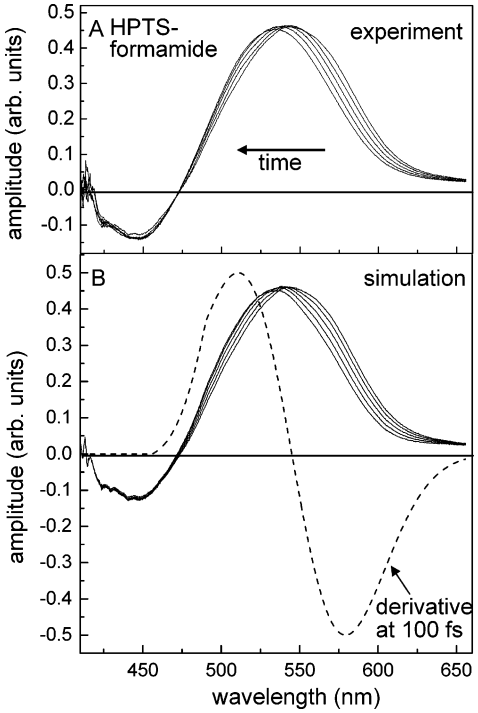

Figure 2. (A) Experimental pump−probe spectra for HPTS in formamide at 100 and 600 fs and 2, 4, and 300 ps. The positive peak at 550 nm is due to excited-state absorption and the negative peak at 450 nm is due to stimulated emission. The time-dependent Stokes shift is evident. (B) Simulated pump−probe spectra constructed, for each time, by taking a linear combination of the initial pump−probe spectrum (100 fs) and its derivative (dotted line) to reproduce the Stokes shift.

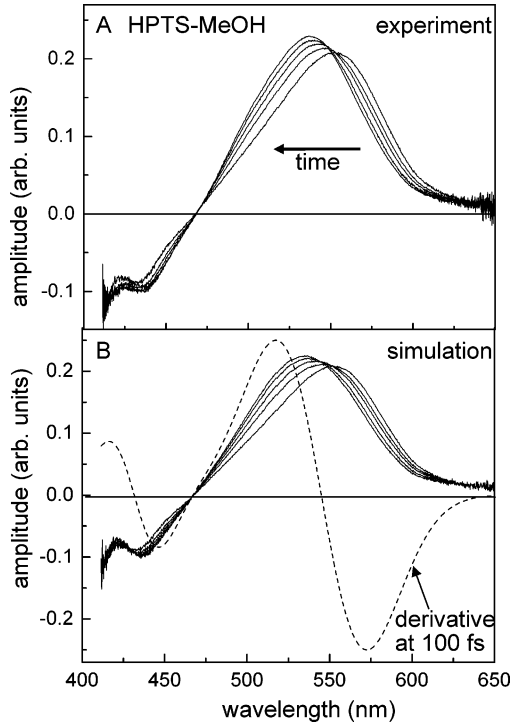

Figure 3. (A) Experimental pump−probe spectra for HPTS in methanol at 1, 4, 9, 20, and 180 ps. (B) Simulated pump−probe spectra constructed, for each time, by taking a linear combination of the initial pump−probe spectrum (100 fs) and its derivative (dotted line) to reproduce the Stokes shift.

From our findings in other solvents, it seems fairly universal that the frequency shift is substantially larger for excited-state absorption than stimulated emission. In fact, in the case of formamide and the other systems studied here besides methanol, stimulated emission shows little Stokes shift. It can also be seen that both the peak shape and oscillator strength (or peak area) are approximately conserved throughout the Stokes shift in the formamide solvent (Figure 2A). The excited-state absorption maximum peak height in methanol increases slightly with time, but the peak width decreases in a proportionate manner (Figure 3A).

Starting from the initial spectrum, and given the nature of the observed Stokes shifts, it is possible to quite accurately model and reproduce the observed spectral dynamics. If a peak shifts a small amount relative to its width, then the time-dependent shift can be described by a first-order expansion relative to its original position. The time-dependent spectrum can then by modeled as a linear combination of the initial spectrum with its derivative with respect to frequency.

$$f(\omega,t) \cong f(\omega_0) + \Delta\omega(t) f'(\omega_0) \tag{2}$$

$\Delta\omega(t)$ is a multiplicative factor that determines the amplitude of the derivative of the spectrum that is added to the spectrum at each time point. The magnitude of $\Delta\omega(t)$ can be directly equated to the size of frequency shift as a function of time. Figures 2B and 3B demonstrate how eq 1 can be used to reproduce the Stokes shift for formamide and methanol.

First consider formamide (Figure 2). The spectrum is dominated by the excited-state absorption (positive going portion in Figure 2A), and the stimulated emission shows very little Stokes shift as can be seen from Figure 2A. Therefore, the initial excited-state absorption portion of the pump−probe spectrum (taken at 100 fs to avoid any distortions from non-resonant contributions) was fit to a Gaussian. The derivative of the Gaussian is shown in Figure 2B as a dashed curve. The initial spectrum and corresponding Gaussian derivative were then added using a least-squares regression to best reproduce the pump−probe signal at later times. There are two adjustable parameters in the fit, $\Delta\omega(t)$ the multiplicative amplitude factor which determines the spectral shift and an overall scaling factor to match the amplitude of the calculated curve to the data. These two fitting parameters are essentially independent. The progression of calculated curves shown in Figure 2B does an excellent job of reproducing the data in Figure 2A.

The Stokes shift in methanol was the most complicated studied here because the stimulated emission showed a small but non-negligible shift. Therefore, the spectrum at 100 fs was fit as the sum of two Gaussians, one positive (excited-state absorption) and one negative (stimulated emission). The derivative of the fit to the spectrum is shown as the dashed curve in Figure 3B. As with formamide, there are only two adjustable parameters in the fit to reproduce the Stokes shifts of both peaks, that is, $\Delta\omega(t)$ the multiplicative amplitude factor which determines the spectral shift and an overall scaling factor to match the calculated curve to the data. The results are shown in Figure 3B. Again, the agreement is very good, although the peak shape changes somewhat, which was not included in the model.

To compare the fits quantitatively, we can look at the time-dependent frequency correlation function, an empirically defined function given as

$$C(t) = \frac{\nu(t) - \nu(\infty)}{\nu(0) - \nu(\infty)} \tag{3}$$

where $\nu(\infty)$, $\nu(0)$, and $\nu(t)$ are, respectively, the frequencies of the peak maxima at infinite time (the time after the solvent/solute system has reached equilibrium), time zero, and inter-

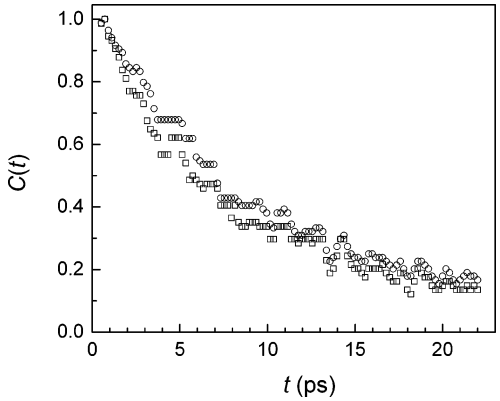

Figure 4. Experimental (squares) and simulated (circles) response function $C(t)$ that describes the time-dependent Stokes shift of the peak of the spectrum for HPTS in methanol.

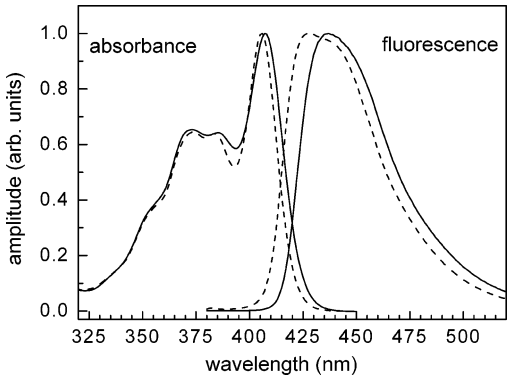

Figure 5. Absorption and fluorescence spectra of HPTS (solid) and MPTS (dashed) in glycerol. The spectra are almost identical except that HPTS has a larger steady-state Stokes shift.

mediate times t. Figure 4 displays the $C(t)$ decay curves resulting from the experimental data (squares) and simulated data (circles) for HPTS in methanol. The decays are very similar. Fitting each to an exponential decay, the experimental data gives a 9.3 ps time constant, while the decay time for the simulated data is 9.8 ps.

The time-independent Stokes shift has been well studied for HPTS in a number of solvatochromism studies. A Kamlet−Taft (KT) analysis shows that the magnitude of the frequency shift for fluorescence is highly dependent on specific hydrogen-bonding interactions.[10,23,24] It is then reasonable to compare HPTS with other chromophores that experience similar frequency shifts by specific hydrogen-bonding interactions. The absorption and fluorescence properties of Coumarin 343 (C343) have been examined in a recent solvatochromism study, and it has fairly similar KT parameters as HPTS.[25] $C(t)$ for C343 in methanol has been measured using time-resolved fluorescence studies to be slightly biexponential with a low amplitude short time component of 1.0 ps and a larger amplitude decay of 10.3 ps.[26] The amplitude weighted average of these two numbers gives an average solvation time of 8.6 ps, which is quite similar to the decay time of HPTS in methanol.

More information about the solvation of HPTS can be obtained by considering its methoxy derivative, MPTS. As seen in Figure 5, the absorption and fluorescence spectra of HPTS (solid curves) and MPTS (dashed curves) are very similar. The fluorescence spectrum of HPTS has a larger Stokes shift than MPTS because the electronic structure of the ring is sensitive to the strength of hydrogen-bond donation of the HPTS hydroxyl. This is a common property of photoacids and has been extensively exploited for studying hydrogen-bonding

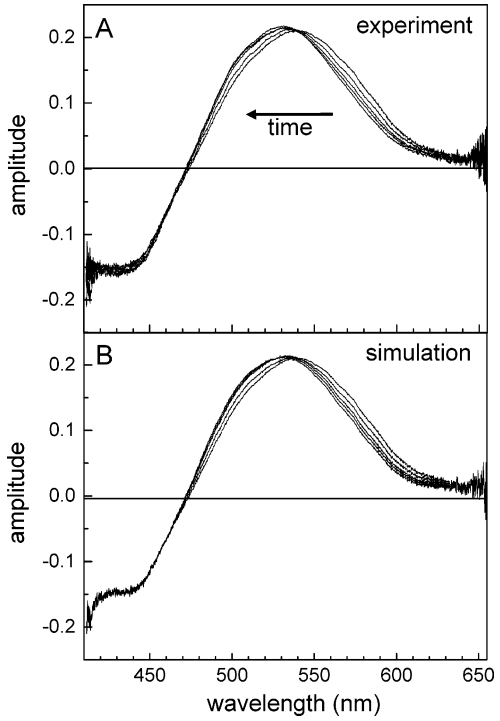

Figure 6. (A) Experimental pump−probe spectra of MPTS in water at 100 and 600 fs and 2, 4, and 300 ps. The Stokes shift is fast. (B) Simulated spectra pump−probe spectra at the same times obtained using the same method as that discussed for Figure 2B. The simulated results are in very good agreement with the data.

systems.[1,2] However, even though the maximum frequencies do not precisely coincide, the peak shapes and widths are quite similar.

The experimental pump−probe spectra of MPTS in water are shown in Figure 6A. The data sets are at 100 and 600 fs and 2, 4, and 300 ps. Note that the Stokes shift is much faster in water than in methanol. By 4 ps, the long time limit has approximately been reached. Many more data points were acquired and will be discussed below. The same technique used in modeling the spectral shift of HPTS in methanol and formamide is used to simulate the experimental data in Figure 6B. Just as the time-independent Stokes shift is much smaller for MPTS than HPTS (see Figure 5), the time-resolved frequency shift is much more modest for MPTS in water than for HPTS in formamide or methanol. Even though the amplitude of the frequency shift is less for MPTS in water than what should be expected for HPTS in water, it is reasonable to assume that the solvation time scales will be the same for both molecules in a given solvent. This is a general assumption of linear response theory, and moreover, we measured no appreciable difference in the decay of $C(t)$ in MPTS relative to HPTS in methanol. Furthermore, as noted above, the time scale of the Stokes shifts of C343 and HPTS in methanol are the same. As mentioned previously, in water, the solvation response is much faster than in methanol. The increased rate is consistent with fluorescence up-conversion studies of C343 in water that show the solvation dynamics to have two components, an inertial component of ∼100 fs and a slower component of ∼900 fs.[27,28] In the current experiments, we did not use sufficient time resolution to measure a ∼100 fs component. The measured $C(t)$ of MPTS in H_2O gives a 990 fs decay constant. These results on MPTS in water suggest that we would expect HPTS in water to exhibit a ∼1 ps Stokes shift.

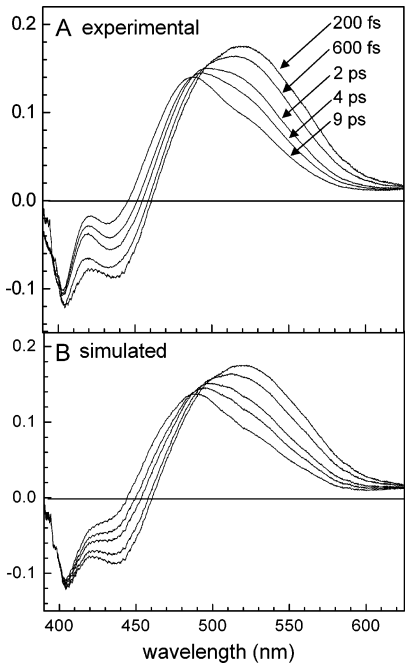

Figure 7. (A) Experimental pump−probe spectra of HPTS in water. In the first several picoseconds, there is a decrease in both excited-state absorption (520 nm) and stimulated emission (440 nm). This is consistent with a deprotonation of HPTS. The peak at 400 nm corresponds to the ground-state bleach. (B**)** Simulated spectra pump−probe spectra at the same times as those shown in **A** using eq 3. Both the Stokes shift and the deprotonation are reproduced accurately by the calculations.

B. HPTS in Water−Stokes Shift and Proton Transfer. In contrast to HPTS in formamide or methanol, photoexcitation of HPTS in water leads to deprotonation. Figure 7A shows data taken on HPTS in water at relatively short times. Notice the substantial difference in the data compared with HPTS in formamide (Figure 2A) or MPTS in water (Figure 6A), which have dynamics on similar time scales. As stated above, the act of simple solvation responsible for the Stokes shift almost conserves the peak shape and area, neither of which is conserved in the first several picoseconds following excitation of HPTS in water. Instead, there is a significant peak shape change and roughly equivalent decrease in signal for both excited-state absorption (positive going) and stimulated emission (negative going). The only part of the pump−probe spectrum that does not show a decrease in amplitude is the negative peak at ∼400 nm, which is due to a ground-state bleach. A proton-transfer process does not return HPTS to the ground state, so this peak is expected to keep the same amplitude in the course of excited-state proton transfer.

A method related to the model used to describe the Stokes shift dynamics of HPTS and MPTS in solvents where proton transfer does not occur can be used to describe the entire time dependence of the HPTS spectrum including separating the Stokes shift from the deprotonation dynamics. Taking the pump−probe spectrum at all times to be described by a linear combination of the protonated and deprotonated states of HPTS, the spectra can then be reconstructed by three spectral basis functions: one representing the protonated population, one representing the deprotonated population, and one which describes the time-dependent Stokes shift. The pump−probe signal can then be expressed as

$$S_{PP}(\omega,t) = \alpha(t)f_{HA}(\omega) + \beta(t)f'_{HA}(\omega) + (1 - \alpha(t))f_{A^-}(\omega) \quad (4)$$

The protonated state pump−probe spectrum, $f_{HA}(\omega)$, is given by the spectrum at $t \cong 0$. The deprotonated state pump−probe spectrum, $f_{A^-}(\omega)$, is represented by the very long time spectrum. The solvation is incorporated through the derivative of the protonated state spectrum, $f'_{HA}(\omega)$, as previously described in section III.A. In practice, $f_{HA}(\omega)$ is taken to be equal to the experimental pump−probe signal at 100 fs to avoid spectral distortions from the non-resonant contribution that occurs for $t \sim 0$. The deprotonated spectrum is taken at 600 ps, which is after the vast majority of deprotonation has occurred. In this approach, the entire time dependence is carried in the coefficients $\alpha(t)$ and $\beta(t)$, where $\alpha(t)$ reflects the extent of proton transfer and $\beta(t)$ accounts for the Stokes shift. Note that there are only two adjustable parameters.

The simulated data using eq 3 is shown in Figure 7B. The agreement with the experimental spectrum is excellent for the times shown, especially when one considers only two parameters are varied to reproduce the experimental spectrum. The experiments were conducted in both H_2O and D_2O over a wide range of times. Only a portion of the data taken in H_2O is shown in Figure 7.

Figure 8 shows data for a much wider range of times for HPTS in D_2O. Figure 8A shows the three basis functions used in reconstructing the data. The shifting function is almost identical to the one used to model the Stokes shift of MPTS in water. The Stokes shift time dependence is contained in $\beta(t)$ (eq 3), which is related to $\Delta\omega(t)$ in eq 2 by $\Delta\omega(t) = \beta(t)/\alpha(t)$. $\beta(t)$can be used to compute the time-dependent frequency correlation function, $C(t)$ (see below), even though it cannot be directly observed for HPTS in water due to the competing proton-transfer process. Figure 8B shows the experimental data (black curves) over the entire spectrum, 410−620 nm, over a range of times. At 520 nm, the curves are, from top to bottom, 100 and 600 fs and 2, 9, 20, 50, 90, 180, 300, and 500 ps. The red curves are the fits to the data using eq 4. The agreement between the fits and the data is truly excellent over the entire wavelength range with two adjustable parameters. Furthermore, as discussed below, after the first few picoseconds, the Stokes shift is over, and then there is only one adjustable parameter, the ratio of the protonated to deprotonated spectra. Figure 8C is an expanded view of the data and the fits centered at ∼525 nm. This figure shows very clearly the ability of the calculations using eq 4 to reproduce the data quantitatively on all time scales.

The fits provide the dynamics of two time-dependent processes, the Stokes shift and the deprotonation. Through the use of eq 4, these are readily separated. Figure 9 shows the Stokes shift data for MPTS in water (circles). These points were obtained from analyzing data as illustrated in Figure 6 using eq 3. Figure 6 shows only a small number of the many time-dependent spectra that were recorded and analyzed. The solid curve is for HPTS in water obtained from the analysis of data like those shown in Figure 8 using eq 4. The results are almost identical. The HPTS and MPTS data were fit as single-exponential decays. The fits give a time constant for the Stokes shift of HPTS in H_2O of 950 and 990 fs for MPTS in H_2O. The results in D_2O also have reasonable agreement, with the MPTS and HPTS Stokes shift time constants being 1.7 and 1.5 ps, respectively. The similarities of the Stokes shifts obtained for HPTS and MPTS further confirm the ability to analyze the experimental data and separate the HPTS Stokes shift from the deprotonation kinetics. The observed deuterium isotope effect for the Stokes shift is in reasonable agreement with studies of C343, which measure a time constant in D_2O of roughly be 30% longer than that in H_2O.[29,30]

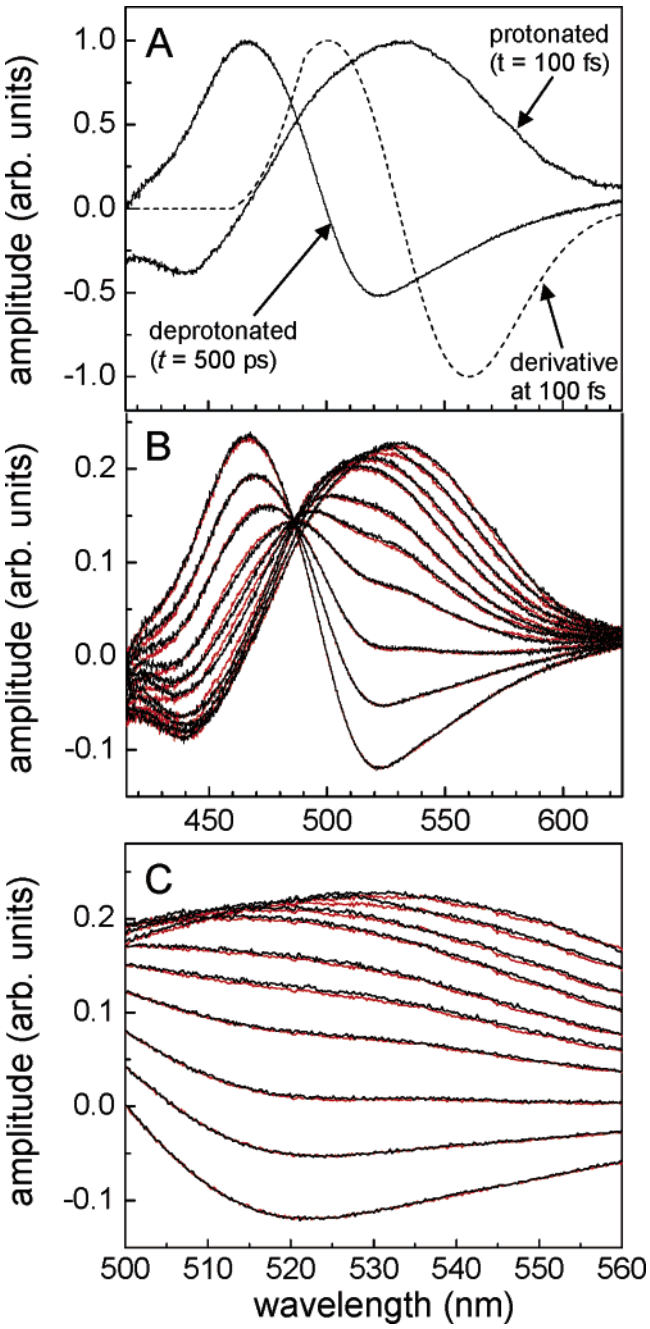

Figure 8. (A) Three spectral components used to reproduce the time-dependent pump−probe spectra for HPTS in D_2O. (B) The simulated pump−probe spectrum for HPTS in D_2O at 100 and 600 fs and 2, 9, 50, 90, 180, 300, and 500 ps using eq 3 with the spectra shown in A. Both the Stokes shift and the deprotonation are included in the calculations. The agreement between the data and calculated spectra is excellent. (C) A blowup of B between 500 and 560 nm to display the comparison between the data and the calculations better.

The other time-dependent parameter in eq 4, $\alpha(t)$, describes the extent of proton transfer. It is the probability that the initially prepared protonated HPTS excited state is still protonated at time t. Because of the nature of the analysis, $\alpha(t)$ only carries information about the extent of proton transfer and is uncoupled from the Stokes shift dynamics. The decay of $\alpha(t)$ is shown in Figure 10 for HPTS in both H_2O and D_2O. Both curves fit well to a biexponential

$$f(t) = a \exp(-t/t_1) + b \exp(-t/t_2) \quad (5)$$

The parameters obtained from the fits to the curves shown in Figure 10 are given in Table 1. Only times up to 150 ps were used in the fits to avoid diffusion effects, which give non-exponential kinetics at long times.[11] The long time scale observation of proton diffusion in the HPTS/water system has been discussed in detail by Huppert and co-workers.[6,7]

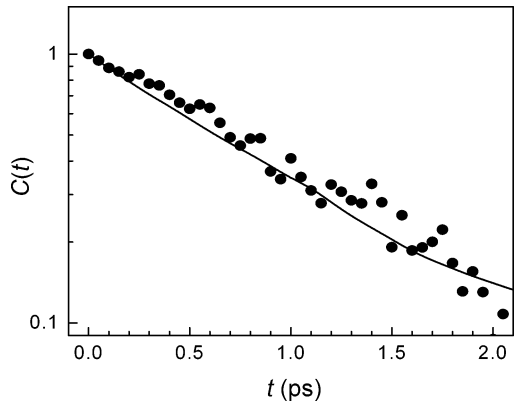

Figure 9. Time-dependent Stokes shift of MPTS in water (points) compared with the Stokes shift of HPTS in water obtained from the calculation of the time-dependent pump−probe spectra using eq 3. Fitting both decay curves to a single exponential gives 950 and 990 fs for HPTS and MPTS, respectively.

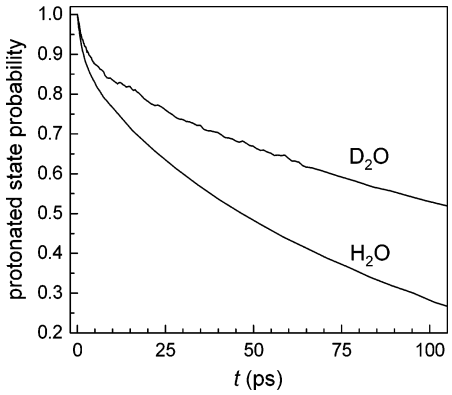

Figure 10. Decay of the protonated state ($\alpha(t)$ in eq 3) for HPTS in H_2O and D_2O. Both curves fit well to a biexponential decay with parameters given in Table 1.

TABLE 1: Protonated State Biexponential Decay Parameters (eq 5)

solvent	a	t_1 (ps)	b	t_2 (ps)
H_2O	0.15	2.5	0.85	88
D_2O	0.15	4.5	0.85	210

The results presented above demonstrate that to obtain the excellent agreement between experiment and calculation displayed in Figures 7−9 requires an accurate description of the ~1 ps Stokes shift and a biexponential (2.5 and 88 ps in H_2O; 4.5 and 210 ps in D_2O) description of the HPTS deprotonation. The biexponential decay constants found for the deprotonation are in relatively good agreement with previous measurements,[11,14] but the quality of the data and fits obtained here indicate that the current numbers are more quantitative. However, the amplitude of the fast deprotonation component is approximately a factor of 2 smaller than previous reports. The difference may occur because earlier experiments did not deal with the Stokes shift in a complete manner. It is possible that part of what is actually the time-dependent Stokes shift was pulled into the fast deprotonation component in the analysis. The quality of the data presented above and the comprehensive approach used here result in quantitative agreement between experiment and calculation as can be seen in Figure 8.

TABLE 2: Parameters Obtained from the Data Using the Two-step Proton-transfer Model (eq 6)

solvent	k_1	k_{-1}	k_2	k_{-2}
H_2O	0.061	0.35	0.07	0.002
D_2O	0.027	0.16	0.03	0.001

The results presented here are in accord with previous electronic spectroscopic studies that found the deprotonation step of HPTS to be a biexponential.[11,14] Experiments that used electronic excitation followed by IR probing of vibrational modes of HPTS report only the long component of the deprotonation.[9] The IR probe experiments might not be expected to be sensitive to the Stokes shift. However, it is clear from the results presented here that the time-dependent Stokes shift is distinct from the biexponential deprotonation kinetics. Apparently, the fingerprint region probed is not sensitive to the short time scale deprotonation dynamics. Below, a model described and applied[11] previously will be used to analyze the biexponential deprotonation. In the model, the first step is the formation of an ion contact pair (fast component) which is followed by the separation of the contact pair into a solvated proton (hydronium ion) and a solvated HPTS anion. The results suggest that the IR probe experiments are sensitive to the second step in this two-step process but not the first.

The two-step proton-transfer scheme given by eq 1 leads to the following coupled rate equations.

$$\begin{pmatrix} \frac{d[AH\cdots B]}{dt} \\ \frac{d[A^-\cdots HB^+]}{dt} \\ \frac{d[A^- + HB^+]}{dt} \end{pmatrix} = \begin{pmatrix} -k_1 & k_{-1} & 0 \\ k_1 & -(k_{-1}+k_2) & k_{-2} \\ 0 & k_2 & -k_{-2} \end{pmatrix} \begin{pmatrix} [AH\cdots B] \\ [A^-\cdots HB^+] \\ [A^- + HB^+] \end{pmatrix} \quad (6)$$

Starting with the initial condition that all species present are in the protonated state at time zero, [AH···B] is equal to $\alpha(t)$ in eq 4. The rate constants are then obtained by fitting the solution for [AH···B] in the above rate equations to the decay curves for $\alpha(t)$ shown in Figure 10. Because the basis function representing the deprotonated state taken at 600 ps still has a small contribution from the protonated state, the long time offset for the fit was obtained from time-correlated single photon counting fluorescence data. The results are given in Table 2, which are similar to those found in previous studies.[11,14] The ratio between the initial deprotonation and recombination rate constants give the quasi-equilibrium rate constant of ~0.16, which is established in the first few picoseconds and reflects the magnitude of fast time deprotonation decay (*a* in Table 1). The forward rate constants k_1 and k_2 are of comparable size to one another. The second reverse rate constant k_{-2} is quite small and contains a large uncertainty because the data is fit only over the initial 150 ps to avoid diffusion kinetics. Since k_{-2} dictates the long time offset to the exponential decay, it contains a larger error than the other rate constants because the analysis is truncated at a relatively short time.

IV. Concluding Remarks

A comprehensive study of photoinduced deprotonation of HPTS in H_2O and D_2O has been presented using visible pump−probe spectroscopy and a method of analysis that accurately takes into account the time-dependent Stokes shift of the HPTS spectra. The method for obtaining the Stokes shift is demonstrated on HPTS in solvents that do not permit deprotonation and on MPTS (methoxy derivative, see Figure 1) in water, which does not undergo deprotonation. Through the use of the new method of analysis (eq 4), it is possible to produce the data at all times (Figure 8) very accurately using only the short time pump−probe spectrum (the protonated spectrum), the derivative of the short time spectrum, and the long time pump−probe spectrum (the deprotonated spectrum). Because the decay of the protonated state produces the corresponding increase in the protonated state, all of the data are fit with only two adjustable parameters, one that accounts for the Stokes shift and one that accounts for deprotonation. Therefore, the fits yield separately the time dependence of the Stokes shift and the time dependence of the deprotonation.

The measured time dependence of the Stokes shift component for HPTS in water (1 ps) matches that of MPTS in water. The Stokes shift dynamics of HPTS in methanol and water also are very similar to those that have been reported for the chromophore C343. Once the Stokes shift is separated out, the component of the data that describes deprotonation is biexponential with decay time constants of 2.5 and 88 ps in H_2O and 4.5 and 210 ps in D_2O. The results for the deprotonation times are in agreement with some previous studies that show a biexponential behavior for non-diffusive proton-transfer kinetics.[11,14] However, the magnitude of the fast time component is smaller than previously reported. This difference may be caused by a mixing of the Stokes shift and proton-transfer response when analyzing the time dynamics at a single frequency point in previous studies.

The fast component of the deprotonation[8,11,14] may arise from the Eigen−Weller model for proton transfer.[12,13] In this model, it is produced by the initial deprotonation process that forms a contact ion pair. The second step breaks contact between the two ions. The results presented here are in contrast to visible-pump IR-probe studies, which do not observe the fast component of the deprotonation kinetics and only see the slower ~90 ps decay.[9] Because the experiments and analysis given above unambiguously separate the time dependence of the Stokes shift from the deprotonation dynamics, it is clear that the ~3 ps component of the spectral dynamics is not part of the Stokes shift (~1 ps) and that the deprotonation is biexponential on times short (hundreds of picoseconds) compared with diffusive contributions.

Acknowledgment. This work was supported by the Department of Energy (DE-FG03-84ER13251). D. B. Spry thanks the National Science Foundation for an NSF Fellowship.

References and Notes

(1) Elsaesser, T.; Bakker, H. J. *Ultrafast Hydrogen Bonding Dynamics and Proton Transfer Processes in the Condensed Phase*; Kluwer Academic Publishers: Dordrecht, The Netherlands, 2002.
(2) Pines, E. *The Chemistry of Phenols*; Wiley: Chichester, UK, 2003.
(3) Förster, T. *Z. Elektrochem.* **1950**, *54*, 531.
(4) Weller, A. *Z. Phys. Chem.* **1958**, *17*, 224.
(5) Förster, T.; Volker, S. *Chem. Phys. Lett.* **1975**, *34*, 1.
(6) Pines, E.; Huppert, D.; Agmon, N. *J. Chem. Phys.* **1988**, *88*, 5629.
(7) Huppert, D. *Chem. Phys. Lett.* **1986**, *126*, 88.
(8) Prayer, C.; Gustavsson, T.; Tran-Thi, T. H. Fast Elementary Processes in Chemical and Biological Systems; 54th International Meeting of Physical Chemistry, 1996, France.
(9) Mohammed, O. F.; Dreyer, J.; Magnes, B.-Z.; Pines, E.; Nibbering, E. T. *J. Chem. Phys. Chem.* **2005**, *6*, 625.
(10) Tran-Thi, T. H.; Prayer, C.; Millie, P.; Uznanski, P.; Hynes, J. T. *J. Phys. Chem. A* **2002**, *106*, 2244.

(11) Leiderman, P.; Genosar, L.; Huppert, D. *J. Phys. Chem. A* **2005**, *109*, 5965.
(12) Eigen, M.; Kruse, W.; Maass, G.; De Maeyer, L. *Prog. React. Kinet.* **1964**, *2*, 285.
(13) Weller, A. *Prog. React. Kinet.* **1961**, *1*, 187.
(14) Gepshtein, R.; Leiderman, P.; Genosar, L.; Huppert, D. *J. Phys. Chem. A* **2005**, *109*, 9674.
(15) Mataga, N.; Kubota, T. *Molecular Interactions and Electronic Spectra*; Marcel Dekker, Inc.: New York, 1970.
(16) Knochenmuss, R.; Leutwyler, S. *J. Chem. Phys.* **1989**, *91*, 1989.
(17) Knochenmuss, R. D.; Smith, D. E. *J. Chem. Phys.* **1994**, *101*, 7327.
(18) Knochenmuss, R.; Muino, P. L.; Wickleder, C. *J. Chem. Phys.* **1996**, *100*, 11218.
(19) Spry, D. B.; Goun, A.; Fayer, M. D. *J. Chem. Phys.* **2006**, *125*, 144514.
(20) Mohammed, O. F.; Pines, D.; Dreyer, J.; Pines, E.; Nibbering, E. T. J. *Science* **2005**, *310*, 83.
(21) Rini, M.; Magnes, B.-Z.; Pines, E.; Nibbering, E. T. J. *Science* **2003**, *301*, 349.
(22) Rini, M.; Pines, D.; Magnes, B.-Z.; Pines, E.; Nibbering, E. T. J. *J. Chem. Phys.* **2004**, *121*.
(23) Pines, E.; Pines, D.; Ma, Y.-Z.; Fleming, G. R. *Chem. Phys. Chem.* **2004**, *5*, 1315.
(24) Barrash-Shiftan, N.; Brauer, B.; Pines, E. *J. Phys. Org. Chem.* **1998**, *11*, 734.
(25) Correa, N. M.; Levinger, N. E. *J. Phys. Chem. B* **2006**, *110*, 13050.
(26) Tominaga, K.; Walker, G. C. *J. Photochem. Photobiol., A* **1995**, *87*, 127.
(27) Walker, G. C.; Jarzeba, W.; Kang, T. J.; Johnson, A. E.; Barbara, P. F. *J. Opt. Soc. Am. B* **1990**, *7*, 1521.
(28) Jimenez, R.; Fleming, G. R.; Kumar, P. V.; Maroncelli, M. *Nature* **1994**, *369*, 471.
(29) Barbara, P. F.; Walker, G. C.; Kang, T. J.; Jarzeba, W. *Proc. SPIE* **1990**, *18*, 1209.
(30) Pant, D.; Levinger, N. E. *J. Phys. Chem. B* **1999**, *103*, 7846.